

Activation and regulation of endogenous retroviral genes in the human pituitary gland and related endocrine tumours

R. Buslei^{*1}, P. L. Strissel^{†1}, C. Henke[‡], R. Schey[‡], N. Lang[‡], M. Ruebner[‡], C. C. Stolt[§], B. Fabry[‡], M. Buchfelder[¶] and R. Strick[†]

^{*}Institute of Neuropathology, [†]Department of Gynecology and Obstetrics, University-Clinic Erlangen, Lab for Molecular Medicine, [‡]Center for Medical Physics and Technology, University of Erlangen-Nuremberg, [§]University of Erlangen-Nuremberg, Institute for Biochemistry, and [¶]Department of Neurosurgery, University-Clinic Erlangen, Erlangen, Germany

R. Buslei, P. L. Strissel, C. Henke, R. Schey, N. Lang, M. Ruebner, C. C. Stolt, B. Fabry, M. Buchfelder and R. Strick (2015) *Neuropathology and Applied Neurobiology* 41, 180–200

Activation and regulation of endogenous retroviral genes in the human pituitary gland and related endocrine tumours

Aims: Adenohypophysis (AH) hormone-producing cells represent the origin of diverse groups of pituitary adenomas (PA). Deregulation of hypothalamic hormone receptors, growth factors and cAMP signalling have been implicated in the aetiology of PA. Endogenous retroviruses (ERVs) are derived from past exogenous retroviral infections and represent more than 8% of the human genome. Some *ERV* genes encode open reading frames and produce functional proteins, for example, the *ERVW-1* envelope gene *Syncytin-1*, essential for placentogenesis, but also deregulated in human tumours. Data concerning *ERV* expression in the AH and related endocrine tumours are missing. **Methods:** Syncytin-1 protein was analysed in normal AH ($n = 15$) and compared with five PA subtypes ($n = 117$) by immunohistochemistry. Absolute gene expression of 20 *ERV* functional *envelope* genes and *ERVW-5 gag* was measured. PA tissues were examined for Syncytin-1 and the cAMP signalling marker phospho-

CREB-Ser133 using immunohistochemistry. Isolated primary human PA cells were treated with different hormones. Murine embryonic and adult pituitary gland *ERV* expressions were compared with human AH. **Results:** Syncytin-1 protein colocalized with corticotropic cells of AH. In contrast, all PA demonstrated significant Syncytin-1 protein overexpression, supporting deregulation. All other *ERV* genes showed significant up-regulations in different PA subtypes. Phospho-CREB-Ser133 and Syncytin-1 colocalized in PA cells. Cultivated primary PA cells with ACTH or CRH induced their respective receptors and *ERV* genes. *Syncytin-A/-B*, murine orthologues to human *Syncytin-1/-2*, localized to embryonic and adult pituitary glands demonstrating functional mammalian conservation. **Conclusions:** Deregulated *ERV* genes may contribute to PA development via cAMP signalling.

Keywords: adenohypophysis, cAMP, endogenous retrovirus (ERV), pituitary adenoma, Syncytin-1

Correspondence: Reiner Strick, University-Clinic Erlangen, Laboratory for Molecular Medicine, Universitätsstr. 21–23, D-91054 Erlangen, Germany. Tel: +49 9131 85 36671; Fax: +49 9131 85 36670; E-mail: Reiner.Strick@uk-erlangen.de

¹Joint co-authors.

Introduction

The pituitary is a small gland located at the base of the brain in a bony formation called the *sella turcica*. In its function as a key regulator of body homeostasis, the gland is connected to the hypothalamus via the infundibular

stalk through where hormones and different activators and repressors reach the pituitary fossa. Two different lobes with varying functions and distinct anatomical structures can be distinguished: the adenohypophysis (AH, or frontal pituitary lobe/anterior pituitary) and the neurohypophysis (NH, or posterior pituitary lobe/posterior pituitary). The different types of hormone-producing cells in the AH release adrenocorticotrophic hormone (ACTH), thyroid-stimulating hormone (TSH), growth hormone (GH also called STH), Prolactin (PRL), the gonadotrophins luteinizing hormone (LH) and follicle-stimulating hormone (FSH). These hormone-producing cells could be the origin of the vast majority of pituitary tumours so-called pituitary adenomas (PA). They constitute about 10–15% of intracranial neoplasms and represent generally benign lesions [1]. Upon clinical presentation they can be classified as secreting or clinically nonfunctional tumours. One example of hormonal active neoplasms are ACTH-secreting adenomas which cause Cushing's disease, a severe illness associated with overproduction of cortisol and other adrenocorticoids and is associated with multiple clinical complications including hypercoagulability, insulin resistance, hypertension, bone loss and immunosuppression [2,3]. Recently a clinical study involving 343 Cushing's patients and 34 300 controls from the Danish National Registry and Danish Civil Registration System demonstrated that mortality was doubled in Cushing's patients [hazard ratio (HR) 2.3, 95% confidence intervals (CI) 1.8–2.9] compared with controls. Importantly, mortality was due to venous thromboembolism (HR 2.6, 95% CI 1.5–4.7), myocardial infarction (HR 3.7, 95% CI 2.4–5.5), stroke (HR 2.0, 95% CI 1.3–3.2), peptic ulcers (HR 2.0, 95% CI 1.1–3.6), bone fractures (HR 1.4, 95% CI 1.0–1.9) and infections (HR 4.9, 95% CI 3.7–6.4) [3]. Regarding growth hormone (GH) producing PA causing acromegaly, a meta-analysis of 16 studies demonstrated an increased mortality in acromegalic patients compared with the general population as measured by the weighted average of the standardized mortality ratio (SMR) (1.72 with 95% CI 1.62–1.83) [4].

Concerning the molecular aetiology of PA, deregulation of hypothalamic hormone receptors, growth factors, feedback signalling and especially the cAMP pathway have been implicated. Gain of function mutations in the alpha (α) subunit of the heterotrimeric Gs protein have been observed in 30–40% of GH adenomas, 10% clinically nonfunctioning (CINon) adenomas, 5–20% of TSH adenomas and <5% of ACTH adenomas [5]. For example,

gene mutations in Gs α , affecting codons 201 and 222, result in constitutive activity due to the inhibition of GTPase [6]. Additionally, aberrant high wild-type Gs α protein levels as well as unbalanced protein kinase A (PKA) regulatory subunits, overexpression of the cAMP regulatory element-binding protein (CREB) gene and elevated phospho (p)CREB-Serine (Ser)133 have been noted in PA [5]. All of the above indicate that multiple alterations of the cAMP pathway represent one molecular signature for PA.

Endogenous retroviruses (ERVs) are derived from exogenous retroviral infections of germ cells and integrated into the genome of mammals between 0.1 and 40 million years ago [7–9]. More than 8% of the human genome is considered retroviral origin, like retrotransposons, ERVs and elements with ERV origin [10–12]. ERVs, like exogenous retroviruses, code for group-specific antigen (gag), which is a structural protein forming membrane- and self-associations for virus assembly and budding, as well as binding and packaging of RNA strands. Also coded for is a polymerase (pol) encoding the viral enzyme reverse transcriptase (RT) and the viral envelope (env). Most of the ERV genes are nonfunctional due to recombination, mutations and deletions; however, some gag, pol and env from different ERV encode full-length open reading frames and produce functional proteins [13–15]. The env protein contains a surface unit (SU) and a transmembrane domain with an immunosuppressive-like peptide similar to exogenous retroviral env proteins [16]. Up to date 19 different fully coding ERV env genes and two ERV env genes with stop codons from 11 different ERV families are known [13,17]. The env gene of ERVW-1 (chromosome 7q21.2) called *Syncytin-1* was found to be expressed in human placentas and plays an essential role in placentogenesis a process that is controlled by an orchestra of different hormones like LH, FSH and PRL [16,18,19]. The mouse functional homologues of *Syncytin-1* and *Syncytin-2* called *Syncytin-A* and *Syncytin-B*, respectively, were shown to be essential for placentogenesis using knockout mice [20]. ERV env genes have also been implicated in a variety of malignant tumours, for example, breast, endometrium, ovary and testicles where they were aberrantly expressed [17,21–24]. Common to both placental development and tumorigenesis *Syncytin-1* was found up-regulated after cAMP stimulation, either with Forskolin, which induces the adenylate cyclase, or directly with a SP-cAMP analogue indicating positive protein kinase A regulation [25–27].

A few studies have demonstrated ERV expression in the human brain. RNA expression of the *Erv3-1* and the env

gene of *ERVE* were detected in whole brain tissue, but at lower amounts when compared with placenta [28]. *ERVK-102* (chromosome 1q21-q22) and the gag gene of *ERVH* (chromosome 22q12) were found transcriptionally active in normal brain [29]. Furthermore, ERV expression was related to different brain diseases, especially in amyotrophic lateral sclerosis (ALS), in multiple sclerosis (MS) and in diverse mental disorders. For example, brain tissues from autopsy patients with ALS showed increased *ERVK HML-2* and *HML-3 pol* transcripts [30]. Most studies have investigated expression and the functional roles of retrovirus-like structures and RT activity defined as the MS associated retrovirus (MSRV) in patients with MS [31–33]. A high sequence similarity of MSRV with *Syngytin-1* and the env of *ERVW-2* (chromosome Xq22.3) were found [34]. Different ERV expression of *ERVW*, *ERVH*, *ERVFRD*, *ERVE4-1*, *ERVH*, *ERV9* and *ERVK-10* were also detected in serum, cell-free cerebrospinal fluids and brains of schizophrenic patients [35–38].

So far, studies concerning the expression of *ERV* genes in the human pituitary have not been performed. Additionally, the majority of *ERV* env coding genes are either not present or not consistently represented on commercially available microarrays. In this present study, we quantified normal AH tissues and five PA subtypes for the expression pattern of *Syngytin-1* using immunohistochemistry (IHC) and additionally measured 19 codogenic and 1 noncoding *ERV* env genes as well as the *ERVW-5* gag gene using absolute quantitative real-time PCR. Due to the positive correlation of *Syngytin-1* induction with cAMP during placentogenesis and tumorigenesis, we established primary human pituitary adenomas cell cultures to test the influence of different cAMP inducing hormones on *Syngytin-1* and other *ERV* env gene expression. We further analysed for an association of pCREB-Ser133 with *Syngytin-1* using IHC and immunofluorescence on the same AH and PA tissues. Lastly, we tested if RNA of *Syngytin-A* and *Syngytin-B*, murine orthologues to human *Syngytin-1* and *Syngytin-2*, colocalized to the pituitary glands of embryo day E18.5 and adult mice.

Materials and methods

Patient subjects and AH adenomas

The following study concept was approved by the Ethical Committee of the University of Erlangen-Nuremberg. Surgical specimens from a total of 187 patients with sellar

lesions were retrieved from the archives of the Department of Neuropathology at the University Hospital of Erlangen. None of the PA used in this analysis were obtained from patients with multiple endocrine neoplasia type I (MEN type I). Each tumour specimen was classified and graded according to the currently valid version of the World Health Organization (WHO) classification system for tumours of endocrine organs using haematoxylin-eosin staining as well as immunohistochemistry (IHC) [1]. Pieces of normal anterior lobe were acquired from patients with sellar exploration, magnetic resonance imaging negative microadenomas, as well as patients with Rathke's cleft cysts served as controls ($n = 15$) (7 men and 8 women, median age 35.5 years). These specimens showed a regular lobulated reticulin fibre network typically observed in the AH and IHC confirmed the regular spectrum of hormone production.

Neuropathological examination and IHC

All biopsy samples were fixed overnight in 4% formalin and routinely processed into liquid paraffin. Sections were cut at 4 µm with a microtome (Microm, Heidelberg), stretched in hot water (60°C) and mounted on positively charged slides (Superfrost + Menzel). The slides were air-dried in an incubator at 37°C overnight. The staining procedure with antibodies against the pituitary hormones was performed using a semiautomated benchmark apparatus (Nexes, Ventana, Illkirch, France) and the Ventana DAB staining system following the manufacturer's recommendations and as described previously [39]. Microwave pretreatment was used when recommended (0.01 M citrate-buffer pH 6.0, 3 min 900 watt and afterwards 2 × 10 min, 250 watt). All slides were counterstained with haematoxylin. For *Syngytin-1* detection, tissue slides were hybridized with the primary antibody overnight at 4°C. *Syngytin-1* IHC was performed on five different adenoma subtypes ($n = 117$) which were grouped according to clinical symptoms due to their hormone release: (i) ACTH: ACTH producing adenoma with clinical signs of Cushing's disease ($n = 19$; 6 men and 13 women, median age 45.5 years); (ii) CINon: clinically nonfunctioning adenoma ($n = 49$; 32 men and 17 women, median age 52 years); (iii) PRL: prolactin producing adenoma ($n = 13$; 8 men and 5 women, median age 43.7 years); (iv) Acro: adenoma with clinical signs of acromegaly ($n = 29$; 13 men and 16 women, median age 40.7 years); and (v) TSH: TSH producing adenoma ($n = 7$; 2 men and 5 women,

median age 38 years). IHC of all surgical specimens was performed using the following panel of antibodies and respective dilutions: ACTH (1:2000, mouse, clone 02A3, DAKO, Glostrup, Denmark), FSH [1:500, mouse, clone AB-3 (FSH03), Thermo Fischer Scientific, Waltham MA, USA], hGH (1:100, mouse, clone 54/9 2A2, Biogenex, Fremont CA, USA), LH [1:2000, mouse, clone Ab-1 (LH01), Thermo Fischer Scientific, Waltham MA, USA], PRL [1:5000, mouse, clone AB-2 (PRL02), Thermo Fischer Scientific, Waltham MA, USA], TSH [1:500, mouse, clone 0042, DAKO, Glostrup, Denmark], Syncytin-1 (1:1000, rabbit polyclonal, Imgenex, San Diego, CA, USA).

Additional antibodies used for IHC experiments were: (i) monoclonal antibodies (1:20 dilution) specific for TGF- β 1 (MAB240, R&D) and TGF- β 3 (MAB243, R&D) performed with two paraffin tissue sections of PA (CINon and ACTH) and a term human placenta; and (ii) pCREB-Ser133 (Millipore, polyclonal antibody, 1:1000) with PA ($n = 6$) and AH ($n = 1$).

Evaluation of IHC staining

The immunohistological staining pattern of Syncytin-1 expression was analysed and scored unaware of any diagnosis concerning the hormonal status of patients. Results were assessed semiquantitatively as the per cent of positive cells and described as the following: Normal AH biopsies served as controls and were scored according to the number of Syncytin-1 immunoreactive cells in each sample (0–100%) and the intensity of Syncytin-1 immunoreactivity (graded 0–3); grade 0 = no expression, + = low intensity, ++ = distinct intensity, +++ = vast intensity (like pituicytes in NH). In the same way Syncytin-1 expression scores for every single tumour were calculated according to the number of positive cells and the intensity of immunoreactivity in relation to Syncytin-1 expression in normal AH (graded 0–4, with 0 meaning no stained cells; + = lower intensity than majority of pituitary cells; ++ = similar intensity than majority of pituitary cells; +++ = higher intensity than majority of pituitary cells; ++++ = vast intensity). Thereafter a quotient for every group and marker was calculated, setting 0 = 0, + = 1, ++ = 2, +++ = 3 and ++++ = 4, and divided by the number of samples [40,41].

IHC of both pCREB-Ser133 and Syncytin-1 were performed using separate tissue sections and then analysed in the same regions from PA ($n = 6$) and AH ($n = 1$). Four

40- μ m squared regions were analysed for the percentage of strong, intermediate, weak and negative pCREB-Ser133 nuclei expression and then compared with the amount of Syncytin-1-positive cells in the same tissue region.

Double immunofluorescence staining

Selected tissue sections were incubated overnight with primary antibodies directed against Syncytin-1 (Imgenex, rabbit polyclonal 1:100) or Syncytin-1 monoclonal mouse antibody (mab) 14A5 against the SU (1:350), kind gift from Dr H. Perron (Geneuro, Geneva, Switzerland), in conjunction with either pCREB-Ser133 (1:1000), or antibodies against different anterior lobe hormones including ACTH, (mab DAKO, 1:2000), FSH (mab Thermo, 1:500), hGH (mab Sigma/Aldrich, 1:800), LH (mab Thermo, 1:2000), PRL (mab Thermo, 1:5000) and TSH (mab DAKO 1:500) at 4°C and then subsequently detected with fluorescence labelled secondary anti-rabbit antibodies conjugated with carbocyanine (Cy)2 (diluted 1:200, Jackson ImmunoResearch/Dianova, Hamburg, Germany) or anti-mouse Cy3 (diluted 1:50, Jackson ImmunoResearch/Dianova, Hamburg, Germany). Cell nuclei staining was performed using Hoechst 33342 (Sigma-Aldrich, Schnelldorf, Germany) for 5 min at room temperature. Slides were analysed using an Olympus BX-51 fluorescent microscope (Olympus, Hamburg, Germany) equipped with an F-View II CCD camera (Soft Imaging System, Stuttgart). All secondary antibodies were tested separately and showed no specific cellular immunolocalization.

Confocal laser scanning microscopy

Confocal microscopy (Leica SP5X) was performed on selected tissue sections as indicated above, which showed colocalization of Syncytin-1 and normal AH hormone-producing cells (ACTH). Primary antibodies included Syncytin-1 and ACTH. Secondary antibodies for Syncytin-1 were a goat anti-rabbit Cy2 detected with an Ar-laser at 488 nm and an ACTH goat anti-mouse Cy3 detected with a He-Ne-laser at 543 nm. Laser power was set to approximately 1.2 mW in order to avoid extensive photobleaching. To localize Syncytin-1 on primary adenoma cells, following 72 h of culturing cells on glass coverslips coated with FCS, the cells were fixed with paraformaldehyde 4%, washed with 1 \times PBS, treated with 5% horse serum and 1% BSA in 1 \times PBS for 1 h and then

incubated overnight in a humid chamber at 4°C with the Syncytin-1 antibody. Cells were washed with 1× PBS, incubated for 1 h at room temperature with a Cy2 antibody then washed with 1× PBS and the nuclei stained with DRAQ5 (Biostatus Lim., UK) according to manufacturer's instructions. Cy2 was detected with an Ar-laser at 488 nm and DRAQ5 with a He-Ne laser at 633 nm. The Cy2 secondary antibody solely was negative for any immunolocalization. All 3D imaging processing was performed using the AMIRA (Burlington, MA, USA). For all top view 3D images, raw images were selected and a volume rendering was performed to visualize the dimensionality of the samples.

Murine brain preparation

Pregnant wild-type mice or adult mice of the C57BL/6J and C3H strains were kindly provided from the research group of Dr Wegner, Institute of Biochemistry of the University Erlangen-Nuremberg. Animal experiments were performed in strict accordance with the protocol, which were approved by the Committee on the Ethics of Animal Experiments of the University of Erlangen-Nuremberg (Permit Number: TS-00/12). Whole pituitary glands from adult brains or total whole mouse brains from E18.5 mice were fixed in 4% PFA for frozen sections for 1 h or overnight respectively. Samples were washed six times in 1× PBS, perfused with 30% sucrose overnight, embedded in Tissue-Tek (Sakura, Hartenstein, Germany) and stored at −80°C.

In situ hybridization (ISH) of murine brain sections

Digoxigenin (DIG)-labelled antisense and sense RNA probes were generated for *Syncytin-A* and *Syncytin-B* according to Henke *et al.* [42]. Plasmids were linearized with restriction enzymes and RNA probes were transcribed and DIG-labelled using a RNA-Labeling Kit (Roche, Germany). Twelve-micrometre tissue pituitary sections were obtained from adult pituitary glands (cross-sections) ($n = 2$) and from a whole E18.5 mouse brain (sagittal sections) [43]. Tissue sections were hybridized with *Syncytin-A* and *Syncytin-B* probes using ISH according to Henke *et al.* [42]. Lastly, ISH tissue sections were counterstained with nuclear fast red (Sigma-Aldrich) and mounted in Mowiol (Roth, Germany).

RNA, cDNA preparation and absolute quantitative real-time PCR (qPCR)

Snap frozen human tissue samples were retrieved from our tissue bank (−80°C). Control samples of the human pituitary gland were collected from autopsies ($n = 8$; *post mortem* interval ranged from 12 to 36 h). From all tissues, frozen sections were microscopically reviewed to confirm neoplastic growth or absence of tumour growth respectively. Total RNA was extracted from 30–50 mg of frozen tissues according to Strick *et al.* [26]. cDNA, ERV env primers and qPCR of 20 ERV env genes [*Syncytin-1* (ERVW-1), *Syncytin-2* (ERVFRD-1), *Syncytin-3* (ERVpB), *Erv3-1-1* (ERV3-1), *envE4-1* (ERVE4-1), *envH1-3* (p62, p60, p59), *envV-1* (ERVV-1), *envV-2* (ERVV-2), *envFc1* (chromosome Xq21.33), *envFc2* (ERVFC1-1), *envRb* (ERVpALB-1), *envK-1-7* (ERVK-1-7 in addition to *envK-1-6* the primer also recognized *envK-102*, which has only a partial codogenic env) and *envW-2* (ERVW-2)] were used according to [17,44]. We differentiated between *Syncytin-1*, *envW-2* and the env of MSRV by choosing discriminatory primer pairs according to Mameli *et al.* [45] and Strissel *et al.* [17]. In addition, ERVW-5 gag (p30) on chromosome 3q26.32 (AF156961) was analysed quantitatively with the following primer: cloning primers TF (AGATGTATTCTGGAG AATTGGGACCAA) and BR (ATCAATATAGCCGTCAGG GTTATCTGA) and for real-time PCR: TF (AGGGCAAAT GGAGTGAAGTG) and BR (GGACTCTGAGGGCTTCCTGT). Regarding primary PA cell cultures described below, RNA was fractionated, purified, DNaseI treated and then cDNA was synthesized according to Strissel *et al.* [46]. Semiquantitative real-time PCR (Applied BioSystems 7300) using a SYBR green-based master mix (Thermo Scientific) was performed with cDNA (40 ng/well) and primers for the human *CRHR1* (TF: 5' CACGTCTGA GACCATTCACTACA; BR: 5' ACGAAGAACAGCATGTA GGTGAT); *CRHR2* (TF: 5' ACCTACATGCTCTTCTTCG TCAAT; BR: 5' CTGCAGGAAGGAGTTGAAATAGAT) and *ACTHR* (TF: 5' ATCACACTGACCATCCTGCTC; BR: 5' TTCACCTGGAAGAGAGACATGTAG). Normalized $2^{-\Delta\Delta CT}$ values for RNA gene expression were calculated according to Strissel *et al.* [46], where co-amplification of the housekeeping gene 18S-rRNA was used for normalization in semiquantitative analysis.

Snap frozen mouse adult pituitary glands ($n = 6$) were retrieved from −80°C and then RNA was isolated and processed the same as described above. cDNA, mouse ERV env

primers and qPCR of *Syncytin-A* and *Syncytin-B* were according to Henke *et al.* [42].

Primary cell cultures

Three human adenoma primary tissues were obtained from the Institute of Neuropathology, Erlangen, including (i) an atypical densely granulated GH adenoma from a patient with clinical signs of acromegaly (Acro); (ii) a corticotrophic cell adenoma from a patient suffering from Cushing's disease (ACTH); and (iii) a gonadotroph cell adenoma with FSH and LH expression (CINon). A single tissue piece from each PA was frozen at -80°C and used for analyses of protein expression. The remaining tissue sample was used for cell culture involving cAMP induction experiments. Briefly, the adenoma tissue was washed with $1\times$ PBS, cut into small tissue pieces and digested in a solution containing collagenase (1 mg/ml) for 1.5 h on a rotator at 37°C . Trypsin was added at a final concentration of 0.02% for an additional 30 min with frequent microscopic monitoring. The cell suspension was washed and centrifuged at 179 g until the supernatant cleared. Cell pellets were resuspended and plated into T25 tissue culture flasks and maintained in RPMI medium supplemented with 10% FCS, non-essential amino acids, L-glutamine and 1% penicillin/streptomycin. Following 5 days after initial set-up the cellular supernatants were collected and tested for expression of hormones FSH, LH, PRL and hCG using ELISA (Dxl 600; Beckmann Coulter GmbH, Krefeld, Germany) in the Endocrinology Laboratory, Department of Obstetrics and Gynecology, and ACTH and GH at the Neuroendocrinology Laboratory, Department of Neurosurgery both at the University Hospital, Erlangen. For cAMP induction experiments, at day 5 following set-up of initial short term cell cultures the cells were trypsinized and divided into 12-well culture dishes (200 000 cells per well) in RPMI medium with 5% charcoal treated serum (CTS). Sixteen hours later hormones and the known cAMP stimulator Forskolin were added to cell cultures at the concentration: ACTH (2×10^{-9} M), CRH (0.5×10^{-9} M) and Forskolin (4×10^{-5} M). The RNA was harvested 48 h later to analyse *ERV* gene expression. In addition, primary cells grown on coverslips were treated with either ACTH or Forskolin and then stained with a membrane-specific wheat germ agglutinin conjugated with Alexa594 and nuclei-specific Hoechst 33342 and analysed by microscopy according to Ruebner *et al.* [47]. All primary placental villous trophoblasts were

isolated and cultured according to our past publications [44,47].

Statistical analyses

The nonparametric Mann–Whitney *U* test for independent samples was performed using IBM SPSS Statistics 21 (IBM, Germany). For all tests a *P* value: <0.05 was considered as statistically significant. For each mean value, a standard error of the mean (s.e.m.) was calculated using IBM SPSS Statistics 21.

Results

Human Syncytin-1 protein was expressed in normal AH and significantly overexpressed in PA

To determine if Syncytin-1 was expressed in human AH, we performed IHC on tissue sections of normal pituitary. Interestingly, Syncytin-1 expression revealed a variable degree of reactivity in epithelial cells throughout the AH. For example, in the *pars intermedia* a specific Syncytin-1-positive cell population showed a very strong granular cytoplasmic staining pattern with a predominance of basophil cell clusters (Figure 1). To further characterize this cell population, we performed double immunofluorescence staining with antibodies against Syncytin-1 and the most important hormones produced in the AH (ACTH, FSH, GH, LH, PRL and TSH). Only ACTH and Syncytin-1 antibodies showed a distinct but not exact overlap using confocal microscopy (Figure 2). This result supports that hormone producing corticotrophic cells of the normal AH shows a distinct Syncytin-1 expression.

We then asked the question, if Syncytin-1 protein was also detectable in PA ($n = 117$) and whether there were differences in the expression levels between tumour subgroups and the AH. Therefore, five different hormone producing tumour classes (ACTH, CINon, PRL, Acro, TSH) comprising 117 different cases were analysed. Results showed that in contrast to 15 control tissues (AH), Syncytin-1 protein expression was deregulated and associated with all hormone producing neoplastic cells. A calculated overall score of 1.586 ± 0.06 was determined for the control group (Figure 1, Table 1), whereas the calculated mean value scores of the PA groups, from the lowest to highest Syncytin-1 expression, were: 1. CINon = 2.289 ± 0.04 ; 2. TSH = 2.314 ± 0.10 ; 3. PRL = 2.361 ± 0.13 ; 4. Acro = 2.562 ± 0.06 ; and 5. ACTH = 2.568 ± 0.05 .

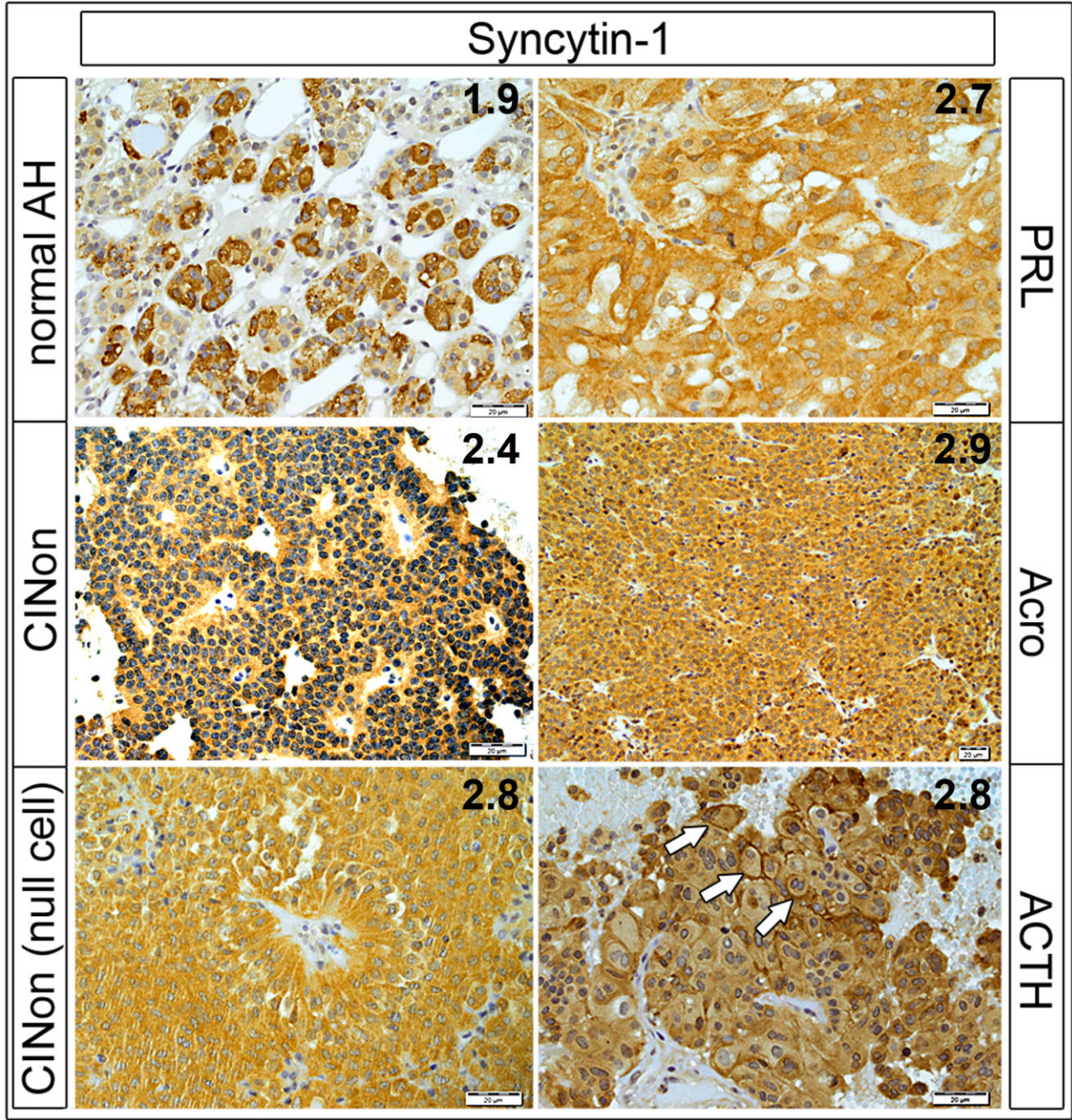


Figure 1. IHC of Syncytin-1 expression in the normal AH and various PA. Five different PA subtypes are shown; CInon was an LH producing adenoma. Note the clonal expansion of Syncytin-1 expression throughout each tumour type. Arrows in the ACTH adenoma show examples of strong membrane staining of Syncytin-1. In addition, numbers represent the individual tumour protein expression calculated from IHC (see Table 1). Bars = 20 µm.

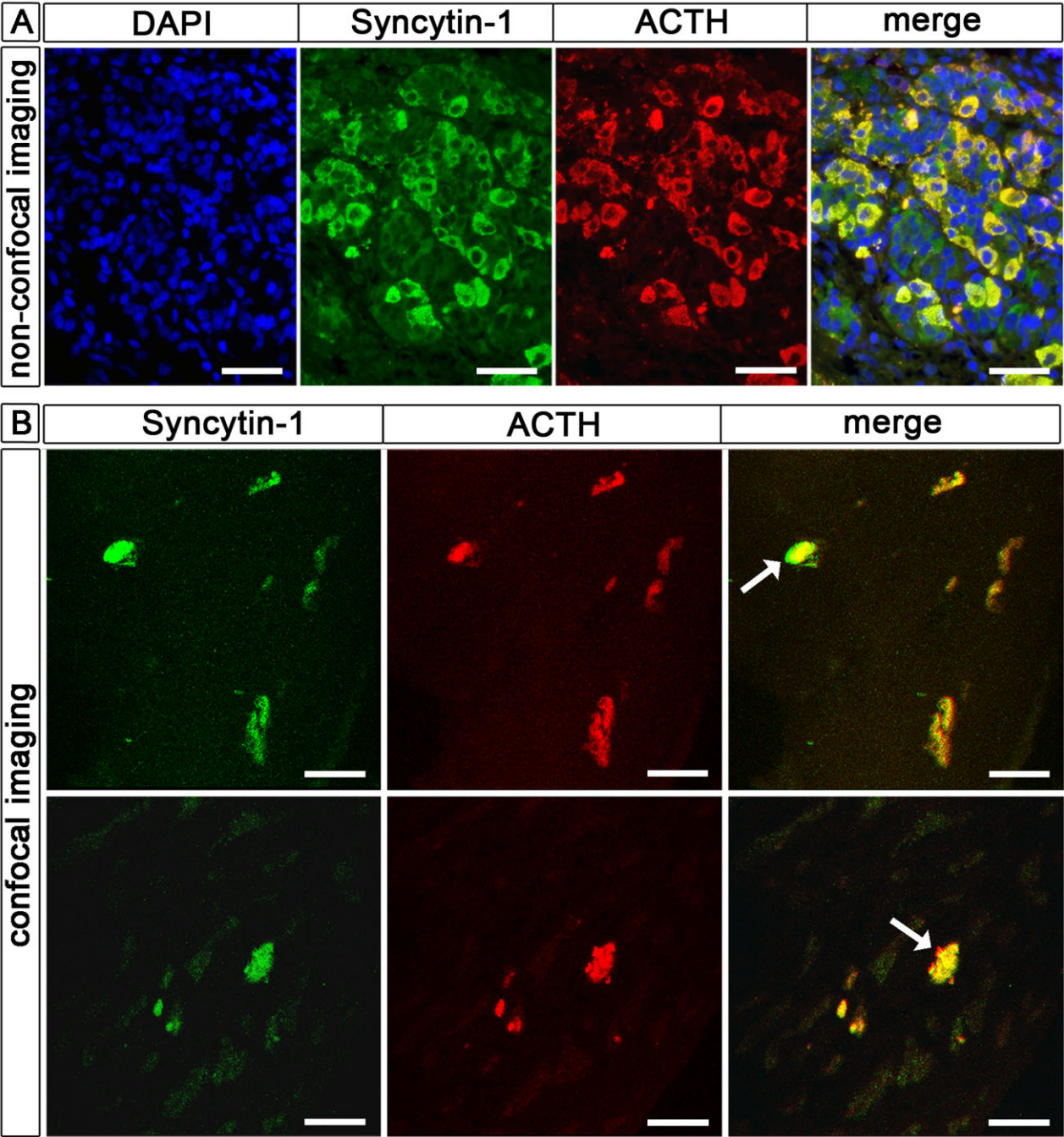
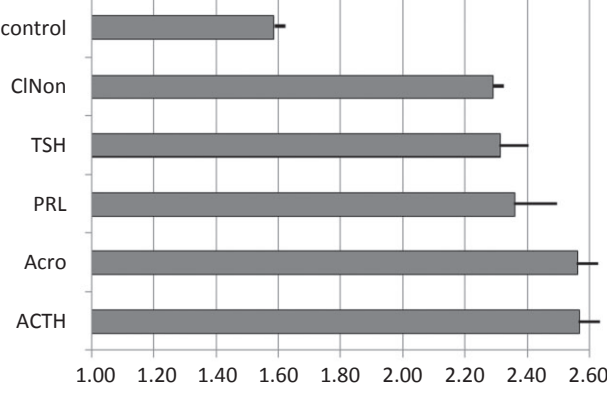


Figure 2. Syncytin-1 and ACTH expression colocalizes to normal AH corticotropic cells. (A) Nonconfocal immunofluorescence images of a normal AH paraffin tissue section showing DAPI staining (blue = nuclei) with cohybridization of primary antibodies specific for Syncytin-1 (green) and ACTH (red) and merged image. Bar = 20 μ m. (B) Confocal microscopy showing immunofluorescence of a normal AH paraffin tissue section cohybridized with primary antibodies specific for Syncytin-1 and ACTH and then detected using an Ar (488 nm) or He-Ne laser (543 nm) respectively. Both top and bottom panels from left to right show a green channel with Syncytin-1, red channel with ACTH localization, a merge of both Syncytin-1 and ACTH. Bar = 40 μ m.

Table 1. Results of the Syncytin-1 IHC analyses

Cohorts	n	Mean \pm SD	P
Control	15	1.586 \pm 0.06	–
CINon	49	2.289 \pm 0.04	<0.0000001
TSH	7	2.314 \pm 0.10	0.000082
PRL	13	2.361 \pm 0.13	0.000108
Acro	29	2.562 \pm 0.06	<0.0000001
ACTH	19	2.568 \pm 0.05	<0.0000001



Cohort	Mean \pm SD
control	1.586 \pm 0.06
CINon	2.289 \pm 0.04
TSH	2.314 \pm 0.10
PRL	2.361 \pm 0.13
Acro	2.562 \pm 0.06
ACTH	2.568 \pm 0.05

Top table shows for each cohort the analysed mean \pm standard error of the mean for the Syncytin-1 protein expression calculated from IHC. The nonparametric Mann–Whitney *U* test for independent samples was performed using IBM SPSS Statistics 21 for calculating the *P* values. Below is a representative graph showing the mean \pm standard error of the mean of Syncytin-1 expression derived from the IHC analyses.

Statistical analysis of Syncytin-1 scores revealed a highly significant increase of Syncytin-1 protein expression for each adenoma group when compared with normal AH (Table 1). No correlation between Syncytin-1 expression and patient age and gender was found. In addition, analysing haematoxylin-eosin stained and Syncytin-1 IHC tissue sections demonstrated no multinuclear cells (greater than or equal to three nuclei) in the normal AH or any of the hormone producing pituitary adenomas, supporting that Syncytin-1 protein expression did not associate with cell fusions.

ERV *env* genes and the ERVW-5 *gag* gene were significantly overexpressed in PA

Due to our significant findings of Syncytin-1 protein overexpression in PA, we initiated RNA expression analyses of a total of 20 ERV *env* genes along with the ERVW-5 *gag* gene using fresh flash frozen adenoma tissues (Figure 3, supplementary Table S1). Absolute quantification of ERV *env* and *gag* gene expression was performed in

an additional adenoma cohort (ACTH = 13, CINon = 52, Acro = 17, PRL = 10; total *n* = 92) including matched adenoma tissues from the same paraffin sections as used from our IHC studies (*n* = 22) and control AH tissues (*n* = 8). Regarding control AH we observed three ERV gene expression groups, one over 100 molecules/ng RNA, one intermediate and one lower than 10 molecules/ng RNA (Supplementary Table S1). In contrast to control AH, all tumour subgroups demonstrated significant deregulated gene expression changes, where Acro tumours showed the most significant increase (Figure 3, supplementary Table S1). For example, 11 ERV genes were either significantly induced [*Syncytin-1* (2.7-fold), *Syncytin-3* (4.3-fold), *Erv3-1* (3.8-fold), *envK-1-7* (3.1-fold), *envT* (3.7-fold) and *ERVW-5 gag* (1.05-fold)] or reduced in expression [*envFc1* (1.9-fold) and *envRb* (1.8-fold)]. Furthermore, in CINon tumours the highest expressed single *env* gene was *Erv3-1* (669.76 \pm 108.38 molecules/ng RNA) (Figure 3, supplementary Table S1).

Murine Syncytin-A and Syncytin-B are conserved in gene expression in E18.5 and adult pituitary glands

As both human *Syncytin-1* and *Syncytin-2* and murine *Syncytin-A* and *Syncytin-B* are functionally homologous we tested if expression in the pituitary gland was conserved through evolution. Hybridizing E18.5 total murine brain tissue and adult pituitary glands with RNA probes for *Syncytin-A* and *Syncytin-B* showed colocalization throughout the cytosol of the pituitary gland (Figure 4). We noted that *Syncytin-A* and *Syncytin-B* gene expression levels were relatively equal in the E18.5. Regarding the adult murine pituitary gland, both *Syncytin-A* and *Syncytin-B* expression was the strongest in the intermediate lobe, weaker in the anterior lobe but only *Syncytin-A* was localized throughout the posterior lobe. In corroboration, *Syncytin-A* and *Syncytin-B* gene expression was also confirmed in adult pituitary glands using qPCR (*n* = 6) (*Syncytin-A*: 43.34 \pm 18.12 molecules/ng RNA; *Syncytin-B*: 73.86 \pm 12.48 molecules/ng RNA (Figure 4).

Stimulation of ERV *env* genes in primary human pituitary adenoma cell cultures following ACTH and CRH hormones and Forskolin treatment

It is well established that upon CRH binding to its receptor in the anterior pituitary gland cAMP signalling is induced

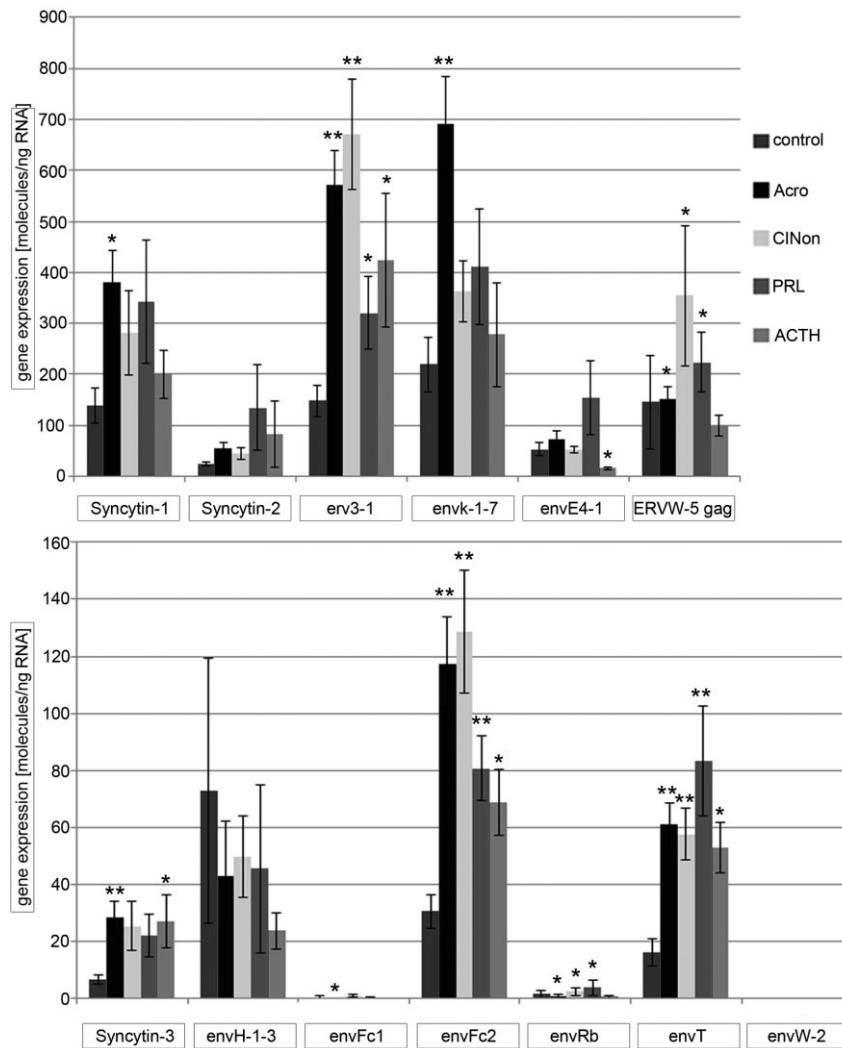


Figure 3. Gene expression of 20 ERV env genes and the ERVW-5 gag in 92 PA and 8 control AH. Top and bottom graphs demonstrate for each PA cohort gene expression (colour coded) values of ERV genes in molecules/ng RNA. The nonparametric Mann-Whitney *U* test for independent samples was performed using IBM SPSS Statistics 21 with **P* < 0.05 significant and ***P* < 0.001 highly significant values. Note that in control AH, *Syncytin-1*, *Erv3-1*, *envK-1-7* and *ERVW-5 gag* were over 100 molecules/ng RNA and represented the highest expressed ERV genes, whereas *Syncytin-3*, *envRb* and *envW-2* were <10 molecules/ng RNA (Table 1). From the highest to the lowest fold induction regarding the Acro PA cohort *Syncytin-1* (2.7-fold), *Syncytin-3* (4.3-fold), *Erv3-1* (3.8-fold), *envT* (3.7-fold), *envK-1-7* (3.1-fold), and *ERVW-5 gag* (1.05-fold) expression were significantly induced compared with the control cohort, whereas *envFc1* (1.9-fold) and *envRb* (1.8-fold) were significantly reduced. The CINon PA cohort showed significant inductions of *Erv3-1* (4.5-fold), *envFc2* (4.2-fold), *envT* (3.5-fold), *ERVW-5 gag* (2.4-fold) and *envRb* (1.6-fold). The PRL cohort showed significant inductions of *envT* (5.1-fold), *envFc2* (2.6-fold), *envRb* (2.6-fold), *Erv3-1* (2.1-fold) and *ERVW-5 gag* (1.5-fold) and the ACTH cohort showed significant inductions of *Syncytin-3* (4-fold), *envT* (3.2-fold), *Erv3-1* (2.8-fold) and *envFc2* (2.2-fold). In contrast, *envE4-1* (3.3-fold) showed significant reduction of expression. Only three genes (*Erv3-1*, *envFc2* and *envT*) were significantly induced in all adenoma cohorts. In contrast to all of the above, *Syncytin-2*, *envH-1-3* and *envW-2* were not significantly deregulated in all PA compared with controls.

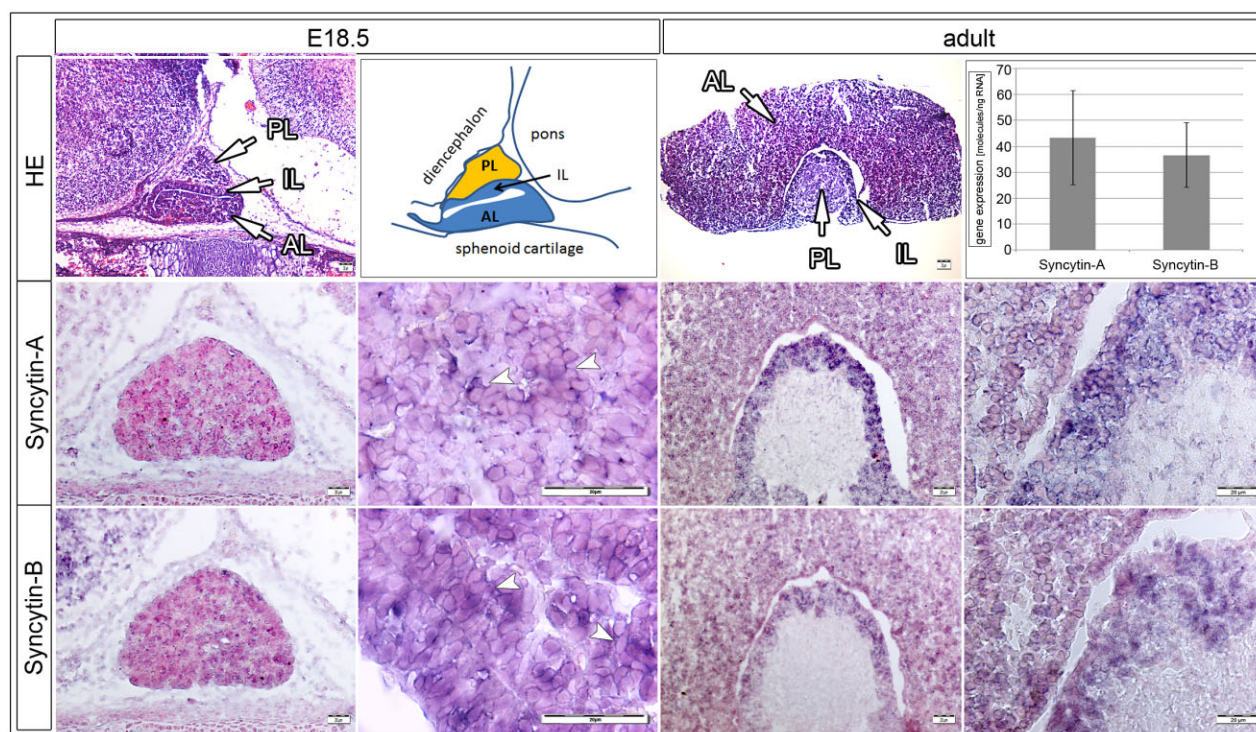


Figure 4. Gene expression of *Syncytin-A* and *Syncytin-B* env genes in E18.5 murine and adult pituitary glands. Top pictures show tissue sections of a whole E18.5 and an adult murine brain stained with haematoxylin-eosin (HE) and a corresponding schematic modified from Sheng and Westphal [48] (PL, posterior pituitary lobe; IL, intermediate pituitary lobe; AL, anterior pituitary lobe). Bottom left and right pictures show magnifications of the pituitary gland from E18.5 murine whole brain sagittal sections and adult pituitary gland cross-sections hybridized with *Syncytin-A* or *Syncytin-B* RNA respectively. Note that the pituitary gland shows the same positive expression for both *Syncytin-A* and *Syncytin-B* in the cytosol (arrows). A graph demonstrating gene expression values of *Syncytin-A* and *Syncytin-B* from six adult murine pituitary glands in molecules/ng RNA is shown at the top right.

leading to ACTH production in corticotrophic cells [5,6]. The literature also demonstrates a positive correlation of cAMP regulation of Syncytin-1 in human placenta and in endometrial carcinomas, as well as by CRH via its receptor in placenta [26,49,50]. Therefore, we asked the question, if *Syncytin-1* and other *ERV env* genes along with the *ERVW-5 gag* gene could be functionally induced upon treatment of primary PA short term cell cultures (Acro, ACTH, CNon) with the hormones ACTH, CRH and Forskolin an adenylate cyclase activator (Figure 5B,C). Additionally, we tested for the gene expression of *ACTHR*, *CRHR1* and *CRHR2*. For comparison primary human placental villous trophoblasts were treated with the same substances.

At the time of initial cell culture set-up, all three primary PA tissues showed Syncytin-1 and Erv3-1 protein expression using immunoblotting (Figure 5A). Similar to normal AH pituitary cell cultures [51] primary PA cells

grew initially in suspension with weak attachment points, but following trypsinization the cells began to grow more attached (Figure 5B). Implementing confocal microscopy and 3D imaging we localized Syncytin-1 to the cellular membrane of a gonadotrophic FSH/LH producing CNon adenoma (Figure 5D,E). From six individual confocal images Syncytin-1 expression showed membrane specificity. 3D reconstruction simulated the same density distribution of Syncytin-1 protein throughout the cell as seen using 2D confocal microscopy. We determined specific levels of PA hormones in supernatants of primary PA short term culture experiments after 5 days, which confirmed each endocrine tumour phenotype (Figure 5C). These initial results of PA expressing Syncytin-1 and ERV-3-1 proteins with Syncytin-1 membrane association, which is similar to the placental syncytiotrophoblast, along with PA hormone secretion represented a basis for functional assays involving ERVs.

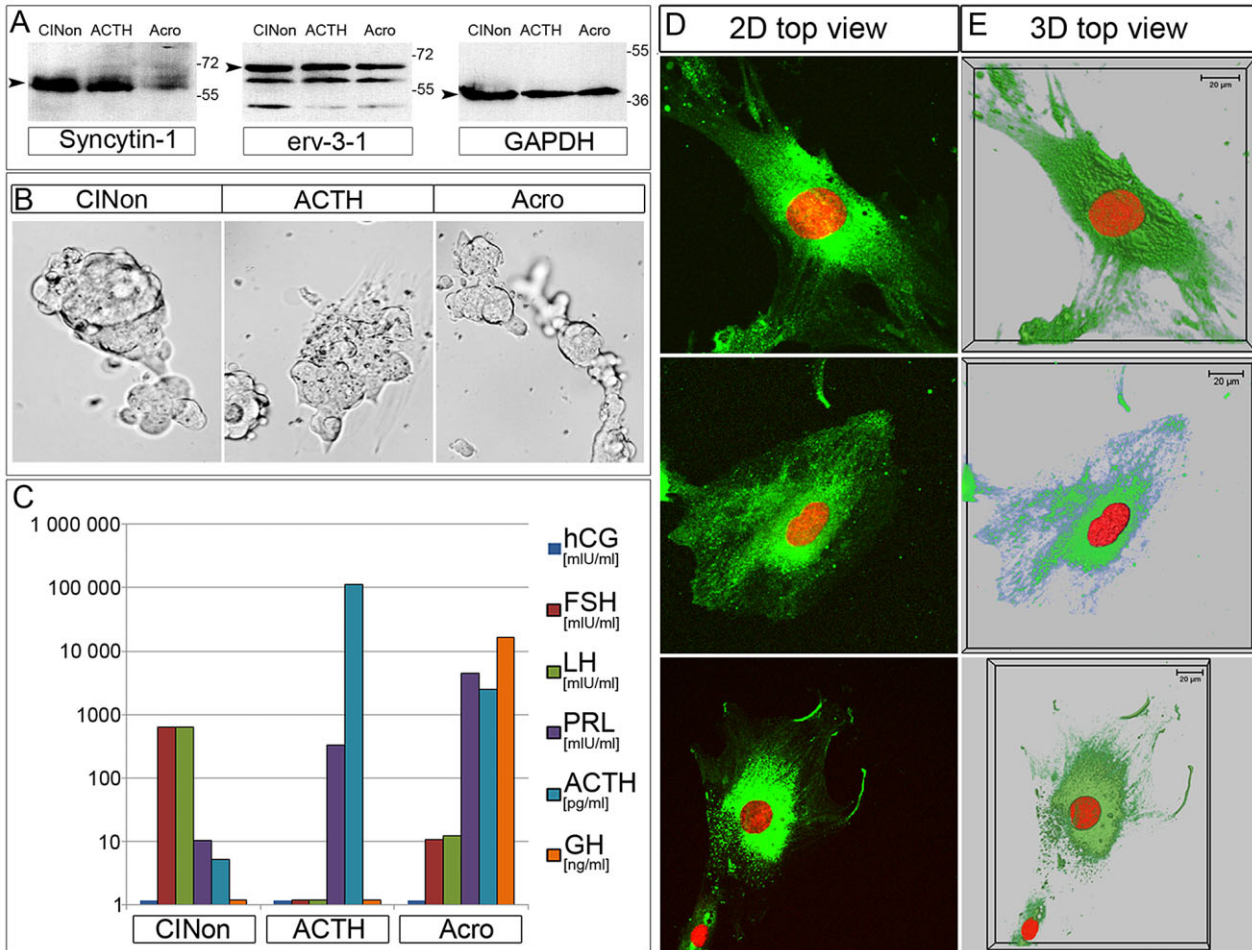


Figure 5. ERV env protein, microscopic and hormonal analyses of PA primary cell cultures. (A) Immunoblot detection of Syncytin-1 and Erv3-1 protein in primary PA from three subtypes at the initial time of collection. Kilodaltons (kDa) are indicated. (B) Primary PA cells of CINon, ACTH and Acro in culture at day 5. (C) Graph shows an indicated serum hormone evaluation of primary PA at day 5 of cell culture. The y-axis represents a logarithmic scale for each indicated hormone value signified in mIU/ml or the specific concentration (pg/ml or ng/ml) as indicated to the right (colour coded). Above each bar on the x-axis the total amount of hormone (mIU/ml or pg/ml or ng/ml) is shown. Note that the gonadotrophic adenoma (CINon) demonstrated the highest FSH (640.6 mIU/ml) and LH (627 mIU/ml) levels while the adenoma cultured from a M. Cushing patient (ACTH) secreted the highest amounts of ACTH (111 813 pg/ml) as well as moderate levels of PRL (336.6 mIU/ml). Additionally, an adenoma cultured from a patient diagnosed with clinical signs of acromegaly (Acro) secreted the highest amounts of GH (16 256 ng/ml) and PRL (4428 mIU/ml) as well as moderate levels of ACTH (2534 pg/ml). (D) Immunolocalization of Syncytin-1 protein expression was analysed from six different microscopically analysed 2D confocal images, each consisting of >25 Z-sections. Pictures show examples of three cells imaging Syncytin-1 on a FSH/LH producing CINon PA. Syncytin-1 antibody was detected using an Ar-laser (488 nm). (E) 2D confocal images constructed into a 3D image according to top view.

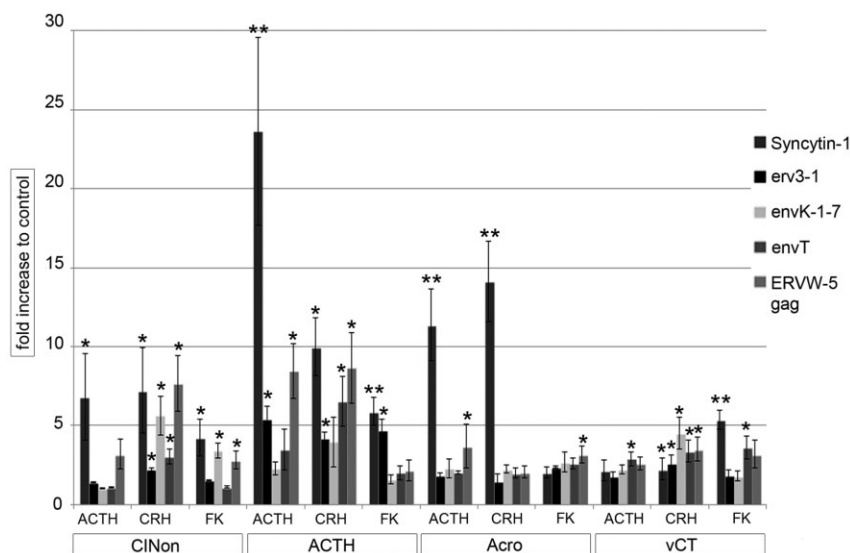


Figure 6. Activation of cAMP with CRH, ACTH and Forskolin of primary PA cell cultures leads to *ERV* gene inductions. Following a 48 h. treatment of primary PA (5% CTS) with ACTH (2×10^{-9} M), CRH (0.5×10^{-9} M) or Forskolin (4×10^{-5} M) *ERV* gene expression was determined in molecules/ng RNA. Graph shows the fold increase above untreated control samples. Specific *ERV* genes are indicated from left to right on x-axis as bars and show the fold increase plus the standard error of the mean above the untreated control sample. For every drug induction a minimum of least three experiments were performed for each PA. In the case of the ACTH PA 10 experiments for each hormone were performed. The nonparametric Mann–Whitney *U* test for independent samples was performed using IBM SPSS Statistics 21 with **P* < 0.05 significant and ***P* < 0.001 highly significant values.

Following 48-h incubation with ACTH and CRH hormones or Forskolin five *ERV* genes were variably increased above control cultures among the tumour types (Figure 6, supplementary Table S2). Results showed that overall the CINon and ACTH PA had the most significant number of *ERV* gene inductions with all three substances, especially CRH, which induced all five *ERV* genes. On the other hand, the Acro PA demonstrated significant induction of either *Syncytin-1* or *ERVW-5 gag* or both genes upon ACTH or CRH treatment; however, only *ERVW-5 gag* was significantly induced after Forskolin. Interestingly, regarding all three PA *Syncytin-1* was the highest induced gene following hormone treatment (Figure 6). Lastly, for all three PA we observed induction of the *ACTHR*, *CRHR1* and *CRHR2* upon hormone treatment (supplementary Figure S1). For example, *ACTHR* and *CRHR1* were induced in PA cell cultures approximately 10-fold in CINon, 5-fold in ACTH and 2-fold in Acro (supplementary Figure S1).

Compared with cultured primary placental villous trophoblasts, PA cultures showed in part higher *ERV* gene inductions after ACTH and CRH treatment. Although Forskolin induced comparable significant *ERV* gene expression levels between PA cells and villous trophoblasts, only a nonsignificant induction for *Syncytin-1* (2.05 ± 0.36 -fold)

was observed in Acro primary cells (supplementary Table S2). Furthermore, treatment of primary PA cells with ACTH or CRH hormones or Forskolin did not result in any multinuclear cells (greater than or equal to three nuclei) (data not shown).

Correlation of *Syncytin-1* and pCREB protein expression in AH and PA

Following our findings supporting a possible co-induction of cAMP signalling with *ERV* genes in primary PA, we asked the question if the cAMP signalling marker pCREB-Ser133 protein was expressed in the same *Syncytin-1* overexpressing PA and AH. Using IHC we demonstrated higher amounts of intermediate and strong positive nuclear pCREB-Ser133 expression in Acro [(*n* = 3) mean = 83.6%]; ACTH [(*n* = 3) 85.6%] and in a single AH [(*n* = 1) 81%]. pCREB-Ser133 expression correlated with over 95% of cells with strong *Syncytin-1* expression in the same PA and with 24.6% strong positive cells in the AH which we deduced were corticotrophic cells as shown in Figure 1 (supplementary Figure S2). Importantly, there were pCREB-Ser133 nuclear expression differences comparing PA with AH. For example, mean values of strongly

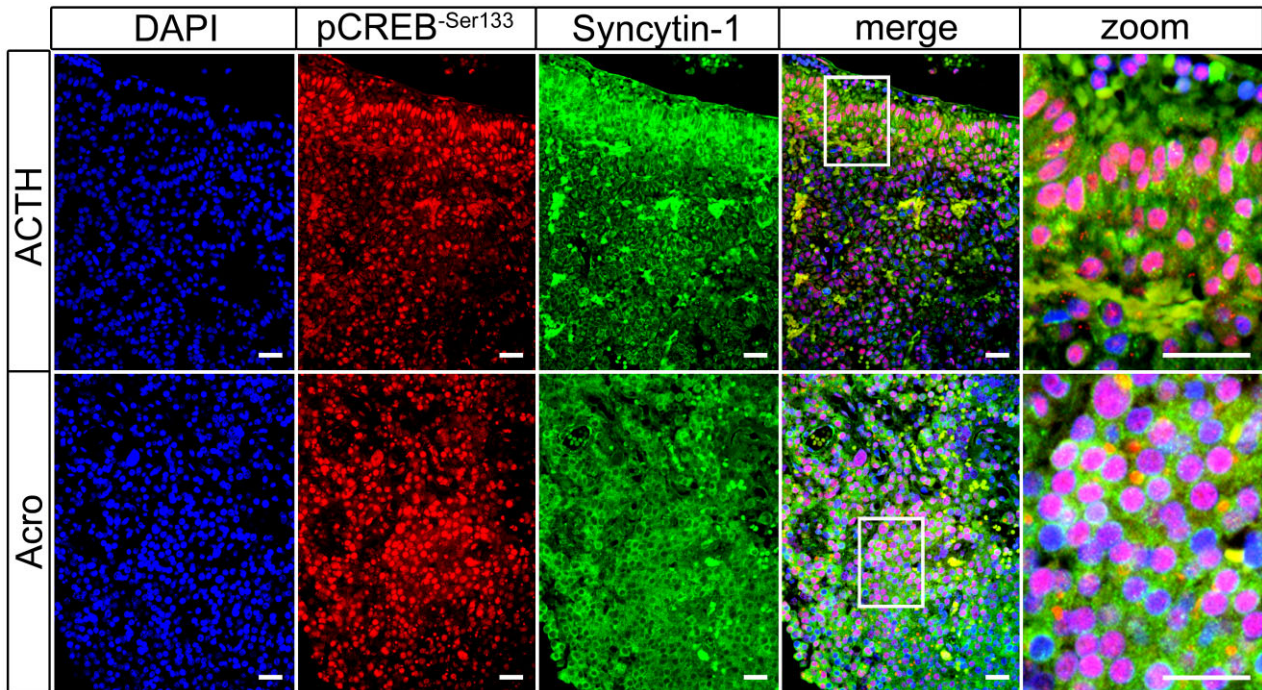


Figure 7. Colocalization of pCREB-Ser133 and Syncytin-1 to the same cells in PA and AH. Nonconfocal immunofluorescence images of one ACTH and one Acro PA paraffin tissue section are shown, with DAPI staining (blue = nuclei), cohybridization of primary antibodies specific for pCREB-Ser133 (red), Syncytin-1 (green) and a merged image. A magnification (zoom) from a part of the merged image (white box) is shown. Note that pink nuclei indicate pCREB-Ser133 positive nuclei (blue plus red), blue nuclei were pCREB-Ser133 negative. Colocalizations of pCREB-Ser133 with Syncytin-1 represent staining of green cytosol/membrane plus pink nuclei. Bar = 20 μ m.

positive nuclei for both ACTH and Acro PAs represented 55.6% and 53.6%, whereas for the AH only 32% was noted. Lastly, it should be noted that all pCREB-Ser133 and Syncytin-1-negative cells represented blood vessels and surrounding stroma (supplementary Figure S2).

In addition to IHC we also performed co-immunofluorescence of pCREB-Ser133 and Syncytin-1 on same PA tissue sections (Figure 7, supplementary Figure S2). Results showed that all three Acro and ACTH PAs showed over 80% colocalization of nuclear pCREB-Ser133 with Syncytin-1 protein expression in the same cells (Figure 7). These findings corroborate our IHC results above and further support a more direct association between deregulated cAMP signalling and induction of Syncytin-1.

Discussion

Pituitary adenomas are detected in approximately 20% of the general population and increase with age irrespective of gender. Although they appear histopathologically benign in the vast majority of cases, they can be highly invasive and even lethal due to infiltration of surrounding

structures. Severe clinical complications from excess hormone production and metabolic effects are frequently seen [52]. PA progression to a carcinoma is rare, but occurs in about 0.1–0.2% of cases [6]. The molecular aetiology of PA is still virtually unknown. Deregulation of signalling pathways mediated by cAMP, growth factors, hormonal stimulation as well as genetic changes have strong implications [5], but there is clearly a need to better understand the molecular basis of PA development. Our investigation points to possible functional roles of *ERV* genes in both human and mouse AH as well as in PA tumorigenesis associated with regulation of cAMP pathway.

In the normal AH we determined a low to high range of RNA molecules for many codogenic *ERV env* genes and the *ERVW-5 gag*, where the highest amounts (>150.00 molecules/ng RNA) were detectable for *Syncytin-1*, *Erv3-1* and *envK-1-7*. We identified positive RNA localization of *Syncytin-A* and *Syncytin-B* to the mouse pituitary gland of E18.5 and adult brains, which indicates conservation through evolution and supports our hypothesis that *ERV* gene expression in the central nervous system goes along with a normal physiological role. This assumption is sup-

ported by other studies where *ERV* gene expression was detected in brain tissues from normal controls and patients with MS as well as other neurological diseases [53–57]. Other investigators also showed RNA expression of *Syncytin-A* in the murine adult brain, the hippocampus as well as total embryonic heads at E11.5 and E15.5. However, these authors did not note the presence of *Syncytin-B* [20].

ERV genes have also been described in several disorders. Irrespective of the origin of MSRV, a potential causal role for Syncytin-1 in MS brain tissue mediating neuroinflammation and death of oligodendrocytes is known [58,59]. In this investigation we demonstrated that seven *ERV env* genes along with *ERVW-5 gag* increased significantly to aberrant levels in a large cohort of human PA, regardless of hormone expression. This observation leads to the assumption that deregulated *ERV env* genes in human AH may play a general role in adenoma formation. Several *ERV* genes have already been strongly implicated with tumorigenesis. The *envK* gene family has been linked to breast cancer and was recently highlighted as stimulating an antigen immune response [60,61]. Treatment with *envK* antibodies of both breast cancer cells in culture and xenograft tumours inhibited growth, supporting a proliferative role of *envK* in these tumour cells [60]. Similarly, a role for Syncytin-1 in mediating steroid hormone proliferative growth of endometrial carcinoma was also demonstrated [26]. Additionally, *envK-1-7* was identified to increase significantly in a step-wise manner from control endometrium to endometrial carcinoma [17]. In line with the above mentioned studies we found a significant 3.1-fold gene overexpression of *envK-1-7* in Acro PA samples compared with controls, thus, pointing to a positive role in the aetiology. The *ERV env* gene (*Erv3-1*) is expressed in many tissues, like testis, skin, thymus, whole brain, placenta and also in a variety of malignomas, like glioma, breast cancer, Wilm's tumour and endometrial carcinoma [13,17,21,28,46]. We found that *Erv3-1* was significantly increased in all four groups of PA under study (GH, CINon, Acro, PRL) compared with controls and represented the highest single expressed *env* gene with up to 669.76 molecules/ng RNA in CINon. This is in line with our recently published observations that control human endometrium had low expression of *ERV env* genes including *Erv3-1*; however, *Erv3-1* became significantly reactivated in endometrial hyperplasia, polyps and endometrial carcinoma, and correlated significantly with tumour grading to a more undifferentiated state

[17]. It was also shown that following transfection of *Erv3-1* expression vectors in the choriocarcinoma cell line BeWo resulted in differentiation changes, increased inter-cellular levels of β -hCG and cAMP [62,63]. Additionally, overexpressing *Erv3-1* resulted in negatively regulating the cell cycle by inhibiting cyclin B and up-regulating the negative regulator p21 [62,63]. Thus, similar to other tumours, *Erv3-1* expression in PA could play a role in controlling differentiation, a speculation that has to be confirmed in further studies.

We especially focused on Syncytin-1 due to its already established relevance noted in MS, carcinogenesis and placentogenesis [16,26,32,56,58]. A detailed Syncytin-1 analysis was performed especially on PA ranging from IHC, gene expression, primary cell cultures and immunofluorescence including confocal microscopy. Syncytin-1 specifically colocalized to corticotropic cells in the human AH. Normal and aberrant expression of Syncytin-1 in AH and several PA subtypes, respectively, were demonstrated due to primers discriminating between *envW-2* and other nonprotein-coding *envW* family members locating on chromosomes 5q11.2, 6q21, 14q21.3, 15q21.3 and 17q21. Importantly, *Syncytin-1* expression was distinctive to MSRV. It is known that the membrane protein of Syncytin-1 is essential for placentogenesis where it mediates villous cytotrophoblasts cell fusion into a syncytia controlling nutrient and gas exchange between the mother and the foetus [16,64–67]. Cell fusion of breast or endometrial cancer cell lines was repressed with antisense RNA or with siRNA against Syncytin-1 respectively [26,68]. For both placental and cancer cell fusions cAMP-signalling has been strongly implicated [26]. Although, Syncytin-1 showed strong membrane localization using IHC and fluorescent microscopy, including confocal microscopy of primary PA cells, no cell fusions (multinucleated cells) in PA tissue sections or in cell culture experiments upon cAMP signalling were found. This could be explained by the abundance of TGF- β 1 and TGF- β 3 proteins (supplementary Figure S3) where it was previously demonstrated that TGF- β negatively regulated cell fusions despite induced Syncytin-1 levels in endometrial carcinoma and placental cell cultures [26]. On the other hand, Syncytin-1 and other fusogenic as well as nonfusogenic *ERV env* genes may have adapted to use the cAMP pathway for different functional roles depending upon the cell type and differentiation state.

Deregulation of the cAMP pathway is one hallmark among hormone-secreting adenomas, although it is still

not known if aberrant cAMP signalling leads to a proliferative advantage of cellular growth [5]. The mitogen-activated protein kinase pathway (MAPK) has also been implicated in PA aetiology, where cAMP cross-talks via ERK1/2 [5]. Interestingly, Forskolin was also shown to induce ERK1/2 activity via cAMP stimulation [5]. In addition to the Forskolin and oestrogen receptor regulatory elements in the *ERVW-1* promoter we also showed that Syncytin-1 gene expression can be regulated via PPAR γ and RXR α , pointing to multiple *ERVW-1* pathway regulations and different functional outcomes [17,25,26,47]. Importantly, cAMP induced Syncytin-1 expression whereas a PKA inhibitor (H89) repressed expression *in vitro*, localizing the DNA response region to the U3 part of the *ERVW-1* LTR promoter [25]. These experiments indicated a cAMP/PKA/CREB regulation pathway for *ERVW-1*. Although only half CRE sites were localized to this region, AP1/AP2/Sp1 binding sites were also found [25]. According to several publications, heterodimers of Fos/Jun and ATF/CREB family members can functionally bind to either TRE or CRE [69,70]. As an example for normal cAMP-dependent PKA regulation in the brain, increased CRH gene expression via CREB occurs in the hypothalamus, results in production of CRH in the paraventricular nucleus, secretion and then binding to the AH CRHR1 with activation of cAMP signalling and ACTH production [5,6,71] (Figure 8). Additionally, the prohormone proopiomelanocortin (POMC) peptide induced from AH corticotrophic cells is cleaved into ACTH, which then binds the ACTHR in the adrenal gland causing the release of cortisol [73]. The ACTHR signals via G-proteins to activate adenylate cyclase and increases cAMP levels [74]. It is intriguing to note that our findings of both *Syncytin-A* and *Syncytin-B* colocalizing to the adult mouse pituitary intermediate lobe corroborates with Mass Spectrometry images of POMC peptides α -MSH and CLIP, supporting a linkage [75]. CRHR, POMC and the ACTHR have also been detected in the placenta [76,77], where we recently demonstrated a sixfold *Syncytin-1* induction of expression in human primary trophoblasts after 48 h of CRH treatment [50]. It was also shown that CRH resulted in the induction of CRHR1 and syncytialization, similar to cAMP alone [78]. Our immunofluorescence and IHC experiments taken together with our primary PA cell culture further corroborates a possible and positive connection between *ERV* gene expression and cAMP signalling. For example, CRH, ACTH and Forskolin treatments resulted in induction of the corresponding

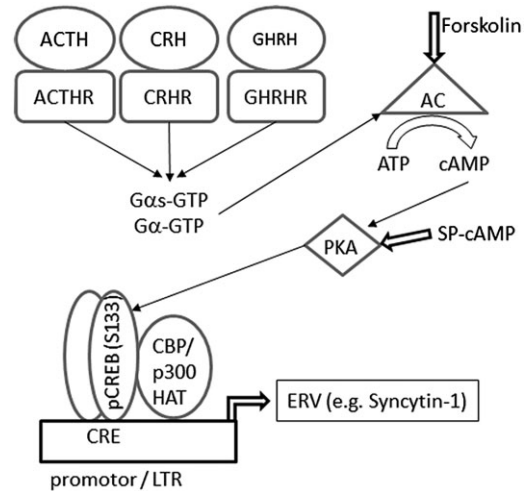


Figure 8. Model shows possible ACTH, CRH and GHRH activation of cAMP leading to ERV promoter regulation by pCREB-Ser133 in PA. Following hormone ligand binding to specific receptors, cAMP levels increase via G-protein (G α s-GTP, G α) and adenylate cyclase (AC). Forskolin also activates the AC. Cellular increased levels of cAMP lead to activation of protein kinase A (PKA) and subsequently phosphorylation of CREB at Ser (S)133. pCREB-Ser133 binds to its nuclear DNA binding site or CREB responsive element (CRE), which was identified important for placental trophoblast function and the *ERV-W1* LTR [47,72].

hormone receptors as well as several *ERV* genes with *Syncytin-1* and *ERVW-5 gag* representing the highest expressed genes. More *ERV* genes were induced by both hormones and Forskolin in CINon and ACTH PA primary cells compared with Acro PA cells, where only *Syncytin-1* and/or *ERVW-5 gag* increased, perhaps relating to different regulations of cAMP signalling. The correlation of over 80% of pCREB-Ser133 and Syncytin-1 double positive PA cells points to a possible co-regulation of Syncytin-1 expression through cAMP signalling, which could help to explain the deregulation of Syncytin-1 in PA. Therefore, we propose a model where general activation and deregulation of cAMP signalling could be one key for understanding ERV activation in PA (Figure 8).

Conclusion

A few studies in the literature have demonstrated *ERV* gene expression throughout brain tissues, except for the pituitary gland and its associated neoplasms. Our study brings forth new information about the expression of *ERV* genes in the normal AH compared with different PA subtypes. Additionally, we demonstrated pituitary gland conservation of *ERV env* expression between humans and

mice. We support the idea that *ERV env* and *gag* gene family members are functional in normal brain including the AH, but become highly induced and deregulated in human PA like in other neoplasms. We could demonstrate that Syncytin-1 colocalized exclusively within ACTH-producing cells in normal AH, but in contrast to all endocrine tumour cells of PA subtypes. Gene expression of *Syncytin-1*, other *ERV env* genes and the *ERVW-5 gag* gene were significantly induced in fractionated primary adenoma cells in the presence of ACTH or CRH hormones. Importantly, the cAMP activated marker protein pCREB-Ser133 and Syncytin-1 colocalized in the same cells from various PA. We present a model whereby *ERV* genes have adapted through evolution to regulate their expression levels via general cAMP signalling thus possibly contributing to aberrant growth or differentiation during tumorigenesis.

Acknowledgements

The expert technical help of Mrs Florentine Koppitz and Verena Schmidt is greatly acknowledged. The authors thank Prof. Wolfgang Saeger, Department of Neuropathology at the University Hospital Hamburg-Eppendorf, Germany, for confirming the diagnosis of the tumour samples. This study was supported by the ELAN at the University Hospital Erlangen to RB. The authors declare that they have no conflict of interest.

Author contributions

Rolf Buslei – study design, experimental work, acquisition and interpretation of data, data analysis.

Pamela L. Strissel – study design, experimental work, data analysis, drafting manuscript.

Christine Henke – experimental work, critical review.

Regina Schey – experimental work, critical review.

Nadine Lang – confocal and 3D experimental work, critical review.

Matthias Ruebner – experimental work, critical review.

Claus C. Stolt – mouse experimental work, critical review.

Ben Fabry – confocal and 3D experimental work, critical review.

Michael Buchfelder – acquisition and interpretation of patient data, critical review.

Reiner Strick – study design, experimental work, data analysis, final manuscript.

References

- 1 deLellis RA. *Pathology & Genetics, Tumours of Endocrine Organs*, Lyon: World Health Organization, IARC Press, 2004
- 2 Asa SL. *Tumours of the Pituitary Gland*, Washington: AFIP, 1998
- 3 Dekkers OM, Horvath-Puho E, Jorgensen JO, Cannegieter SC, Ehrenstein V, Vandenbroucke JP, Pereira AM, Sorensen HT. Multisystem morbidity and mortality in Cushing's syndrome: a cohort study. *J Clin Endocrinol Metab* 2013; **98**: 2277–84
- 4 Dekkers OM, Biermasz NR, Pereira AM, Romijn JA, Vandenbroucke JP. Mortality in acromegaly: a metaanalysis. *J Clin Endocrinol Metab* 2008; **93**: 61–7
- 5 Pertuit M, Barlier A, Enjalbert A, Gerard C. Signalling pathway alterations in pituitary adenomas: involvement of Gsalpha, cAMP and mitogen-activated protein kinases. *J Neuroendocrinol* 2009; **21**: 869–77
- 6 Mete O, Ezzat S, Asa SL. Biomarkers of aggressive pituitary adenomas. *J Mol Endocrinol* 2012; **49**: R69–78
- 7 Dewannieux M, Blaise S, Heidmann T. Identification of a functional envelope protein from the HERV-K family of human endogenous retroviruses. *J Virol* 2005; **79**: 15573–7
- 8 Blaise S, de Parseval N, Benit L, Heidmann T. Genomewide screening for fusogenic human endogenous retrovirus envelopes identifies syncytin 2, a gene conserved on primate evolution. *Proc Natl Acad Sci U S A* 2003; **100**: 13013–18
- 9 Turner G, Barbulescu M, Su M, Jensen-Seaman MI, Kidd KK, Lenz J. Insertional polymorphisms of full-length endogenous retroviruses in humans. *Curr Biol* 2001; **11**: 1531–5
- 10 Bannert N, Kurth R. Retroelements and the human genome: new perspectives on an old relation. *Proc Natl Acad Sci U S A* 2004; **101** (Suppl. 2): 14572–9
- 11 Nelson PN, Carnegie PR, Martin J, Davari Ejtehad H, Hooley P, Roden D, Rowland-Jones S, Warren P, Astley J, Murray PG. Demystified. Human endogenous retroviruses. *Mol Pathol* 2003; **56**: 11–18
- 12 Tristem M. Identification and characterization of novel human endogenous retrovirus families by phylogenetic screening of the human genome mapping project database. *J Virol* 2000; **74**: 3715–30
- 13 de Parseval N, Lazar V, Casella JF, Benit L, Heidmann T. Survey of human genes of retroviral origin: identification and transcriptome of the genes with coding capacity for complete envelope proteins. *J Virol* 2003; **77**: 10414–22
- 14 Villesen P, Aagaard L, Wiuf C, Pedersen FS. Identification of endogenous retroviral reading frames in the human genome. *Retrovirology* 2004; **1**: 32
- 15 Blaise S, de Parseval N, Heidmann T. Functional characterization of two newly identified Human Endogenous Retrovirus coding envelope genes. *Retrovirology* 2005; **2**: 19

- 16 Mi S, Lee X, Li X, Veldman GM, Finnerty H, Racie L, LaVallie E, Tang XY, Edouard P, Howes S, Keith JC Jr, McCoy JM. Syncytin is a captive retroviral envelope protein involved in human placental morphogenesis. *Nature* 2000; **403**: 785–9
- 17 Strissel PL, Ruebner M, Thiel F, Wachter D, Ekici AB, Wolf F, Thieme F, Ruprecht K, Beckmann MW, Strick R. Reactivation of codogenic endogenous retroviral (ERV) envelope genes in human endometrial carcinoma and prestages: Emergence of new molecular targets. *Oncotarget* 2012; **3**: 1204–19
- 18 Blond JL, Beseme F, Duret L, Bouton O, Bedin F, Perron H, Mandrand B, Mallet F. Molecular characterization and placental expression of HERV-W, a new human endogenous retrovirus family. *J Virol* 1999; **73**: 1175–85
- 19 Reis FM, Cobellis L, Luisi S, Driul L, Florio P, Faletti A, Petraglia F. Paracrine/autocrine control of female reproduction. *Gynecol Endocrinol* 2000; **14**: 464–75
- 20 Dupressoir A, Marceau G, Vernochet C, Benit L, Kanellopoulos C, Sapin V, Heidmann T. Syncytin-A and syncytin-B, two fusogenic placenta-specific murine envelope genes of retroviral origin conserved in Muridae. *Proc Natl Acad Sci U S A* 2005; **102**: 725–30
- 21 Cohen M, Kato N, Larsson E. ERV3 human endogenous provirus mRNAs are expressed in normal and malignant tissues and cells, but not in choriocarcinoma tumor cells. *J Cell Biochem* 1988; **36**: 121–8
- 22 Larsson LI, Holck S, Christensen IJ. Prognostic role of syncytin expression in breast cancer. *Hum Pathol* 2007; **38**: 726–31
- 23 Wang-Johanning F, Frost AR, Johanning GL, Khazaeli MB, LoBuglio AF, Shaw DR, Strong TV. Expression of human endogenous retrovirus k envelope transcripts in human breast cancer. *Clin Cancer Res* 2001; **7**: 1553–60
- 24 Wang-Johanning F, Liu J, Rycak K, Huang M, Tsai K, Rosen DG, Chen DT, Lu DW, Barnhart KF, Johanning GL. Expression of multiple human endogenous retrovirus surface envelope proteins in ovarian cancer. *Int J Cancer* 2007; **120**: 81–90
- 25 Prudhomme S, Oriol G, Mallet F. A retroviral promoter and a cellular enhancer define a bipartite element which controls env ERVWE1 placental expression. *J Virol* 2004; **78**: 12157–68
- 26 Strick R, Ackermann S, Langbein M, Swiatek J, Schubert SW, Hashemolhosseini S, Koscheck T, Fasching PA, Schild RL, Beckmann MW, Strissel PL. Proliferation and cell-cell fusion of endometrial carcinoma are induced by the human endogenous retroviral Syncytin-1 and regulated by TGF-beta. *J Mol Med* 2007; **85**: 23–38
- 27 Chang CW, Chuang HC, Yu C, Yao TP, Chen H. Stimulation of GCMA transcriptional activity by cyclic AMP/protein kinase A signaling is attributed to CBP-mediated acetylation of GCMA. *Mol Cell Biol* 2005; **25**: 8401–14
- 28 Andersson AC, Yun Z, Sperber GO, Larsson E, Blomberg J. ERV3 and related sequences in humans: structure and RNA expression. *J Virol* 2005; **79**: 9270–84
- 29 Nakamura A, Okazaki Y, Sugimoto J, Oda T, Jinno Y. Human endogenous retroviruses with transcriptional potential in the brain. *J Hum Genet* 2003; **48**: 575–81
- 30 Douville R, Liu J, Rothstein J, Nath A. Identification of active loci of a human endogenous retrovirus in neurons of patients with amyotrophic lateral sclerosis. *Ann Neurol* 2011; **69**: 141–51
- 31 Perron H, Lalande B, Gratacap B, Laurent A, Genoulaz O, Geny C, Mallaret M, Schuller E, Stoebner P, Seigneurin JM. Isolation of retrovirus from patients with multiple sclerosis. *Lancet* 1991; **337**: 862–3
- 32 Perron H, Garson JA, Bedin F, Beseme F, Paranhos-Baccala G, Komurian-Pradel F, Mallet F, Tuke PW, Voisset C, Blond JL, Lalande B, Seigneurin JM, Mandrand B. Molecular identification of a novel retrovirus repeatedly isolated from patients with multiple sclerosis. The Collaborative Research Group on Multiple Sclerosis. *Proc Natl Acad Sci U S A* 1997; **94**: 7583–8
- 33 Antony JM, Deslauriers AM, Bhat RK, Ellestad KK, Power C. Human endogenous retroviruses and multiple sclerosis: innocent bystanders or disease determinants? *Biochim Biophys Acta* 2011; **1812**: 162–76
- 34 Laufer G, Mayer J, Mueller BF, Mueller-Lantzsch N, Ruprecht K. Analysis of transcribed human endogenous retrovirus W env loci clarifies the origin of multiple sclerosis-associated retrovirus env sequences. *Retrovirology* 2009; **6**: 37
- 35 Karlsson H, Bachmann S, Schroder J, McArthur J, Torrey EF, Yolken RH. Retroviral RNA identified in the cerebrospinal fluids and brains of individuals with schizophrenia. *Proc Natl Acad Sci U S A* 2001; **98**: 4634–9
- 36 Frank O, Giehl M, Zheng C, Hehlmann R, Leib-Mosch C, Seifarth W. Human endogenous retrovirus expression profiles in samples from brains of patients with schizophrenia and bipolar disorders. *J Virol* 2005; **79**: 10890–901
- 37 Medstrand P, Mager DL. Human-specific integrations of the HERV-K endogenous retrovirus family. *J Virol* 1998; **72**: 9782–7
- 38 Perron H, Mekaoui L, Bernard C, Veas F, Stefas I, Leboyer M. Endogenous retrovirus type W GAG and envelope protein antigenemia in serum of schizophrenic patients. *Biol Psychiatry* 2008; **64**: 1019–23
- 39 Buslei R, Holsken A, Hofmann B, Kreutzer J, Siebzehnruhl F, Hans V, Oppel F, Buchfelder M, Fahlbusch R, Blumcke I. Nuclear beta-catenin accumulation associates with epithelial morphogenesis in craniopharyngiomas. *Acta Neuropathol* 2007; **113**: 585–90
- 40 Lefranc F, Mijatovic T, Decaestecker C, Kaltner H, Andre S, Brotchi J, Salmon I, Gabius HJ, Kiss R. Monitoring the expression profiles of integrins and adhesion/growth-regulatory galectins in adamantinomatous craniopharyngiomas: their ability to regulate tumor adhesiveness to surrounding tissue and their contribution to prognosis. *Neurosurgery* 2005; **56**: 763–76

- 41 Rotondo F, Oniya K, Kovacs K, Bell CD, Scheithauer BW. MAP-2 expression in the human adenohypophysis and in pituitary adenomas. An immunohistochemical study. *Pituitary* 2005; **8**: 75–9
- 42 Henke C, Ruebner M, Faschingbauer F, Stolt CC, Schaefer N, Lang N, Beckmann MW, Strissel PL, Strick R. Regulation of murine placentogenesis by the retroviral genes Syncytin-A, Syncytin-B and Peg10. *Differentiation* 2013; **85**: 150–60
- 43 Kaufmann MH. *The Atlas of Mouse Development*, London: Academic Press, 1998
- 44 Ruebner M, Strissel PL, Langbein M, Fahlbusch F, Wachter DL, Faschingbauer F, Beckmann MW, Strick R. Impaired cell fusion and differentiation in placentae from patients with intrauterine growth restriction correlate with reduced levels of HERV envelope genes. *J Mol Med* 2010; **88**: 1143–56
- 45 Mameli G, Poddighe L, Astone V, Delogu G, Arru G, Sotgiu S, Serra C, Dolei A. Novel reliable real-time PCR for differential detection of MSRVenv and syncytin-1 in RNA and DNA from patients with multiple sclerosis. *J Virol Methods* 2009; **161**: 98–106
- 46 Strissel PL, Ellmann S, Loprach E, Thiel F, Fasching PA, Stiegler E, Hartmann A, Beckmann MW, Strick R. Early aberrant insulin-like growth factor signaling in the progression to endometrial carcinoma is augmented by tamoxifen. *Int J Cancer* 2008; **123**: 2871–9
- 47 Ruebner M, Langbein M, Strissel PL, Henke C, Schmidt D, Goecke TW, Faschingbauer F, Schild RL, Beckmann MW, Strick R. Regulation of the human endogenous retroviral Syncytin-1 and cell-cell fusion by the nuclear hormone receptors PPARgamma/RXRalpha in placentogenesis. *J Cell Biochem* 2012; **113**: 2383–96
- 48 Sheng HZ, Westphal H. Early steps in pituitary organogenesis. *Trends Genet* 1999; **15**: 236–40
- 49 Kudo Y, Boyd CA. Changes in expression and function of syncytin and its receptor, amino acid transport system B(0) (ASCT2), in human placental choriocarcinoma BeWo cells during syncytialization. *Placenta* 2002; **23**: 536–41
- 50 Fahlbusch FB, Ruebner M, Volkert G, Offergeld R, Hartner A, Menendez-Castro C, Strick R, Rauh M, Rascher W, Dotsch J. Corticotropin-releasing hormone stimulates expression of leptin, 11beta-HSD2 and syncytin-1 in primary human trophoblasts. *Reprod Biol Endocrinol* 2012; **10**: 80
- 51 Weiss S, Siebzehrnruhl FA, Kreutzer J, Blumcke I, Buslei R. Evidence for a progenitor cell population in the human pituitary. *Clin Neuropathol* 2009; **28**: 309–18
- 52 Asa SL, Ezzat S. The pathogenesis of pituitary tumors. *Annu Rev Pathol* 2009; **4**: 97–126
- 53 Lefebvre S, Hubert B, Tekai F, Brahic M, Bureau JF. Isolation from human brain of six previously unreported cDNAs related to the reverse transcriptase of human endogenous retroviruses. *AIDS Res Hum Retroviruses* 1995; **11**: 231–7
- 54 Weis S, Llenos IC, Sabunciyan S, Dulay JR, Isler L, Yolken R, Perron H. Reduced expression of human endogenous retrovirus (HERV)-W GAG protein in the cingulate gyrus and hippocampus in schizophrenia, bipolar disorder, and depression. *J Neural Transm* 2007; **114**: 645–55
- 55 Johnston JB, Silva C, Holden J, Warren KG, Clark AW, Power C. Monocyte activation and differentiation augment human endogenous retrovirus expression: implications for inflammatory brain diseases. *Ann Neurol* 2001; **50**: 434–42
- 56 Perron H, Lazarini F, Ruprecht K, Pechoux-Longin C, Seilhean D, Sazdovitch V, Creange A, Battail-Poirot N, Sibai G, Santoro L, Jolivet M, Darlix JL, Rieckmann P, Arzberger T, Hauw JJ, Lassmann H. Human endogenous retrovirus (HERV)-W ENV and GAG proteins: physiological expression in human brain and pathophysiological modulation in multiple sclerosis lesions. *J Neurovirol* 2005; **11**: 23–33
- 57 Nellaker C, Li F, Uhrzander F, Tyrcha J, Karlsson H. Expression profiling of repetitive elements by melting temperature analysis: variation in HERV-W gag expression across human individuals and tissues. *BMC Genomics* 2009; **10**: 532
- 58 Antony JM, van Marle G, Opii W, Butterfield DA, Mallet F, Yong VW, Wallace JL, Deacon RM, Warren K, Power C. Human endogenous retrovirus glycoprotein-mediated induction of redox reactants causes oligodendrocyte death and demyelination. *Nat Neurosci* 2004; **7**: 1088–95
- 59 Antony JM, Ellestad KK, Hammond R, Imaizumi K, Mallet F, Warren KG, Power C. The human endogenous retrovirus envelope glycoprotein, syncytin-1, regulates neuroinflammation and its receptor expression in multiple sclerosis: a role for endoplasmic reticulum chaperones in astrocytes. *J Immunol* 2007; **179**: 1210–24
- 60 Wang-Johanning F, Rycak K, Plummer JB, Li M, Yin B, Frerich K, Garza JG, Shen J, Lin K, Yan P, Glynn SA, Dorsey TH, Hunt KK, Ambs S, Johanning GL. Immunotherapeutic potential of anti-human endogenous retrovirus-K envelope protein antibodies in targeting breast tumors. *J Natl Cancer Inst* 2012; **104**: 189–210
- 61 Wang-Johanning F, Radvanyi L, Rycak K, Plummer JB, Yan P, Sastry KJ, Piyathilake CJ, Hunt KK, Johanning GL. Human endogenous retrovirus K triggers an antigen-specific immune response in breast cancer patients. *Cancer Res* 2008; **68**: 5869–77
- 62 Lin L, Xu B, Rote NS. Expression of endogenous retrovirus ERV-3 induces differentiation in BeWo, a choriocarcinoma model of human placental trophoblast. *Placenta* 1999; **20**: 109–18
- 63 Lin L, Xu B, Rote NS. The cellular mechanism by which the human endogenous retrovirus ERV-3 env gene affects proliferation and differentiation in a human placental trophoblast model, BeWo. *Placenta* 2000; **21**: 73–8
- 64 Dupressoir A, Lavialle C, Heidmann T. From ancestral infectious retroviruses to bona fide cellular genes: role of

- the captured syncytins in placentation. *Placenta* 2012; **33**: 663–71
- 65 Pawelek JM, Chakraborty AK. Fusion of tumour cells with bone marrow-derived cells: a unifying explanation for metastasis. *Nat Rev Cancer* 2008; **8**: 377–86
 - 66 Dittmar T, Schwitalla S, Seidel J, Haverkamp S, Reith G, Meyer-Staeckling S, Brandt BH, Niggemann B, Zanker KS. Characterization of hybrid cells derived from spontaneous fusion events between breast epithelial cells exhibiting stem-like characteristics and breast cancer cells. *Clin Exp Metastasis* 2011; **28**: 75–90
 - 67 Strick R, Beckmann MW, Strissel PL. Cell-cell fusions and human endogenous retroviruses in cancer. In *Cell Fusions*. Ed. L-I Larsson. Dordrecht, Heidelberg, London, New York: Springer Verlag & Business Media, 2011; 395–426
 - 68 Bjerregaard B, Holck S, Christensen IJ, Larsson LI. Syncytin is involved in breast cancer-endothelial cell fusions. *Cell Mol Life Sci* 2006; **63**: 1906–11
 - 69 Hai T, Curran T. Cross-family dimerization of transcription factors Fos/Jun and ATF/CREB alters DNA binding specificity. *Proc Natl Acad Sci U S A* 1991; **88**: 3720–4
 - 70 Matsuo N, Tanaka S, Gordon MK, Koch M, Yoshioka H, Ramirez F. CREB-AP1 protein complexes regulate transcription of the collagen XXIV gene (Col24a1) in osteoblasts. *J Biol Chem* 2006; **281**: 5445–52
 - 71 Itoi K, Jiang YQ, Iwasaki Y, Watson SJ. Regulatory mechanisms of corticotropin-releasing hormone and vasopressin gene expression in the hypothalamus. *J Neuroendocrinol* 2004; **16**: 348–55
 - 72 Strauss JF 3rd, Kido S, Sayegh R, Sakuragi N, Gafvels ME. The cAMP signalling system and human trophoblast function. *Placenta* 1992; **13**: 389–403
 - 73 Slominski A, Zbytek B, Szczesniowski A, Semak I, Kaminski J, Sweatman T, Wortsman J. CRH stimulation of corticosteroids production in melanocytes is mediated by ACTH. *Am J Physiol Endocrinol Metab* 2005; **288**: E701–6
 - 74 Hinkle PM, Sebag JA. Structure and function of the melanocortin2 receptor accessory protein (MRAP). *Mol Cell Endocrinol* 2009; **300**: 25–31
 - 75 Rompp A, Spengler B. Mass spectrometry imaging with high resolution in mass and space. *Histochem Cell Biol* 2013; **139**: 759–83
 - 76 Kalantaridou SN, Makriganakis A, Mastorakos G, Chrousos GP. Roles of reproductive corticotropin-releasing hormone. *Ann N Y Acad Sci* 2003; **997**: 129–35
 - 77 Cooper ES, Greer IA, Brooks AN. Placental proopiomelanocortin gene expression, adrenocorticotropin tissue concentrations, and immunostaining increase throughout gestation and are unaffected by prostaglandins, antiprogestins, or labor. *J Clin Endocrinol Metab* 1996; **81**: 4462–9
 - 78 Chen Y, Allars M, Pan X, Maiti K, Angeli G, Smith R, Nicholson RC. Effects of corticotrophin releasing hormone (CRH) on cell viability and differentiation in the human BeWo choriocarcinoma cell line: a potential syncytialisation inducer distinct from cyclic adenosine monophosphate (cAMP). *Reprod Biol Endocrinol* 2013; **11**: 30
 - 79 Morrish DW, Dakour J, Li H. Functional regulation of human trophoblast differentiation. *J Reprod Immunol* 1998; **39**: 179–95
 - 80 Orsel P, Bielakoff J, De Vernejoul MC. Effects of transforming growth factor-beta on long-term human cord blood monocyte cultures. *J Cell Physiol* 1990; **142**: 293–8

Supporting information

Additional Supporting Information may be found in the online version of this article at the publisher's web-site:

Figure S1. ACTHR, CRHR1 and CRHR2 receptor genes are induced following ACTH and CRH treatment of primary adenoma cells. Following a 48 h. treatment of primary PA cells (5% CTS) with ACTH (2×10^{-9} M) or CRH (0.5×10^{-9} M) or Forskolin (4×10^{-5} M) the respective receptor gene expression was determined. Graph shows the fold significant increase above untreated control samples set to 1. Receptor genes are indicated and show the fold increase plus the standard error of the mean. For every drug induction a minimum of three experiments were performed for each PA. In the case of the ACTH PA 10 experiments for each hormone were performed.

Figure S2. Localization and quantification of pCREB-Ser133 and Syncytin-1 to the same regions in PA and AH using IHC. Two PA (ACTH, Acro) IHC examples are shown from a total of six PA and one AH (pCREB-Ser133 and Syncytin-1). Quantitative analysis was performed with four 40- μ m squared regions per tissue resulting in percentages of strong, intermediate, weak and negative pCREB-Ser133 nuclei expression correlated with Syncytin-1-positive cells in the same region.

Figure S3. Cellular localization of TGF- β 1 and TGF- β 3 within PA and human term placental tissues. Examples of microscopic pictures examples of IHC tissue sections showing TGF- β 1 and TGF- β 3 expression with: CINon PA (top two panels) and ACTH PA (middle two panels). Note the cytoplasmic staining of both TGF- β 1 and TGF- β 3 throughout the PA. TGF- β 1 and TGF- β 3 has been determined to negatively regulate fusion of endometrial carcinoma cell fusion, placenta villous trophoblast cell fusion as well as osteoclast cell fusion [26,79,80]. The bottom

two panels represent TGF- β 1 and TGF- β 3 localization in both human placental villi and the differentiated syncytiotrophoblast (SCT) (arrow) where cell fusion is reduced in the last trimester.

Table S1. Gene expression analyses of 20 different *ERV env* genes and the *ERVW-5 gag* gene in 92 PA and 8 normal AH. From left to right the gene name, control AH gene expression values (molecules/ng RNA) and standard error of the mean (SEM), PA gene expression values (molecules/ng RNA) and SEM with the *P* value indicated below each expression value. All significant values are indicated in bold. The total env molecules/ng RNA per patient cohort is indicated at the bottom above ERVW-5 gag.

Table S2. *ERV* gene stimulation of primary PA cell lines with ACTH, CRH and FK. From left to right columns represent primary cell type cultured including villous cytotrophoblasts (vCT); treatment of cells in 5% CTS with ACTH (2×10^{-9} M), CRH (0.5×10^{-9} M) or Forskolin (4×10^{-5} M); specific *ERV* genes are indicated with the fold increase plus the SEM above the untreated control. The nonparametric Mann–Whitney *U* test for independent samples was performed using IBM SPSS Statistics 21 for *P* value significances (**P* < 0.05 and ***P* < 0.001).

Received 4 October 2013

Accepted after revision 10 March 2014

Published online Article Accepted on 17 March 2014